



ELSEVIER

Available online at www.sciencedirect.com

SCIENCE @ DIRECT®

Journal of Sound and Vibration 283 (2005) 621–643

JOURNAL OF
SOUND AND
VIBRATION

www.elsevier.com/locate/jsvi

Experimental observation of nonlinear vibrations in a rub-impact rotor system

Fulei Chu*, Wenxiu Lu

Department of Precision Instruments, Tsinghua University, Beijing 100084, China

Received 30 July 2003; received in revised form 23 April 2004; accepted 5 May 2004

Available online 5 November 2004

Abstract

An experimental setup is installed to simulate the rotor-to-stator rub of the rotor system. A special structure of stator is designed that can simulate the condition of the full rub. The vibration waveforms, spectra, orbits and Poincaré's maps are used to analyze nonlinear responses and bifurcation characteristics of the system when the rub-impact occurs. Experiments with different conditions, including one and two rotor with single- and multi-disks, are performed. Very rich forms of periodic and chaotic vibrations were observed. The experiments show that the system motion generally contains the multiple harmonic components such as $2X$, $3X$, etc. and the $1/2$ fractional harmonic components such as $1/2X$, $3/2X$, etc. Under some special conditions, the $1/3$ fractional harmonic components such as $1/3X$, $2/3X$, etc. can be observed as well.

© 2004 Elsevier Ltd. All rights reserved.

1. Introduction

Rotor-to-stator rub is a serious malfunction in rotating machinery. It often causes catastrophic failure and subsequent economic loss. Investigation on nonlinear vibrations in a rotor-bearing system with rotor-to-stator rub is very important for the evaluation of the rotating machines' condition and the early prediction of the rub-impact.

*Corresponding author. Fax: +86-10-6278-49.

E-mail address: chufli@mail.tsinghua.edu.cn (F. Chu).

The rotor-to-stator rub is one of the malfunctions occurring often in rotating machinery. It is usually a secondary phenomenon resulting from other faults. When the rub occurs, partial rub can be observed at first. During one complete period, rotor and stator have rub and impact interaction once or a few times. Alternately changed stress is formed in the shaft and the system can exhibit complicated vibration phenomena. Chaotic vibration can be found under some circumstances. Gradual aggravation of the partial rub will lead to full rub and severe vibration makes the normal operation of the machine impossible. Mathematically, the rotor system with rotor-to-stator rub is a nonlinear vibrating system with piecewise linear stiffness. There have been many publications on this problem and relevant topics. Muszynska [1] made a comprehensive review on this problem and gave a list of previous papers on the rub-related vibration phenomena during rubbing. Beatty [2] proposed a mathematical model for rubbing forces with piecewise linear form of stiffness and discussed some important points for diagnosing this fault. Choy and Podavan [3] analyzed the effects of different system parameters on rubbing forces and transient responses while Chu and Zhang [4] discussed the bifurcation and chaotic motion of a rub-impact rotor system. Goldman and Muszynska [5] discussed the thermal effects of the rotor-to-stator rub and their influence on the rotor vibrational response. The heat generated during rotor-to-stator contact stages was calculated as a function of thermal conditions and rotor bow modal parameters. Piccoli and Weber [6] performed an experiment to observe the chaotic motion in a rubbing rotor system. The method of state space reconstruction with delay coordinates was used and Poincaré diagrams, correlation dimensions and Lyapunov exponents were obtained as tools for deciding the existence of chaotic behavior. Edwards et al. [7] investigated the effect of torsion in the numerical analysis of a contacting rotor/stator system. It was found that the torsion had a substantial effect on system response and should not be neglected in models used for the analysis of rub phenomena in rotating machinery. Al-Bedoor [8] discussed the coupled torsional and lateral vibrations of unbalanced rotors including the effect of the rotor-to-stator rubbing. The Lagrangian dynamics was used to obtain the equations of motion, which were then solved using a predictive–corrective time-integration algorithm. He found that the inclusion of the rotor torsional flexibility introduced irregular rubbing orbits when compared with the rubbing orbits obtained using the rotor lateral model. Ding and Chen [9] investigated the non-stationary motion and instability of the shaft/casing system with rubs during passage through the first several critical speeds by using an explicit stable finite difference scheme. Lin et al. [10] discussed the nonlinear behavior of rub-related vibration in rotating machinery. The effects of rotating speed, clearance, damping coefficient, friction coefficient, and boundary stiffness were analyzed. Dai et al. [11] investigated the dynamic behavior of a rotor rubbing with a motion-limiting stop. The stop was found to be effective in the suppression of the violent vibration amplitude of the rotor. Sun et al. [12] discussed a general model of a rub-impact rotor based on the classic impact theory. The Poincaré section, the rotor trajectory, the bifurcation diagram, and the power spectrum were used to reveal the nature of different kinds of motion and it was found that the different chaotic regions showed different configurations of attractors. Feng and Zhang [13] discussed the vibration phenomena of a rotor rubbing with a stator caused by an initial perturbation. They found that in the case of no friction between the rotor and the stator, the full rubbing behaved as forward whirling and when the friction was present the full rubbing behaved as backward whirling. Hu and Wen [14] presented a new method for chaotic

behavior identification of a rub-impact rotor from the measured data with state space reconstruction by delay coordinates and short-term predictability. The method may be helpful for machine condition monitoring and the trend analysis. Zhang et al. [15] investigated the bifurcation and chaotic behavior of the rubbing rotor system varying with the rotating speed and the oil film characteristic parameters. They found that there may be two rubbing regions which were located either near the critical speed or inside the supercritical speed region.

Based on these researches it is not so difficult to judge whether a rotor system has rubbing or not. For partial rub the vibration waveform of the rotor will have truncation. When the rub is developed into full rub, the rotor vibration shows backward orbiting, which is a special feature to identify the rotor-to-stator rub, distinguishing this malfunction from the others. However, for the diagnostics purpose, it is still a difficult task to detect the rubbing position. Wang and Chu [16] presented an experimental method to detect the rubbing location. The method combined the acoustic emission technique with the wavelet transform. The results showed the method to be very effective. Chu and Lu [17] discussed a so-called dynamic stiffness method to detect the rubbing location. The simulation results showed the method to be very effective as well. Peng et al. [18] analyzed the feature extraction of the rub-impact system for the fault diagnostics by means of the wavelet analysis. Similar to this kind of nonlinear system with piecewise linear feature, Hinrichs et al. [19] investigated an impact oscillator and a self-sustained friction oscillator by experiments and numerical simulation. Point-mapping approaches, Lyapunov exponents and phase space reconstruction were used to analyze dynamics of the systems and rich bifurcational behavior was found. Bapat [20] discussed N impact periodic motions of a single-degree-of-freedom oscillator. For some simple cases, exact closed-form expressions were obtained. Effects of amplitude and frequency of sinusoidal force, bias force, damping, and variable and constant coefficients of restitution on periodic motions were investigated. Begley and Virgin [21] investigated the interaction and influence of impact and friction on the dynamic behavior of a mechanical oscillatory system. Dynamical system theory was used as a conceptual framework and comparisons were made between numerical and experimental results over a relatively wide range of parameters.

As a typical malfunction with nonlinear characteristics, the rotor-to-stator rub has very complicated spectrum characteristics and can exhibit very rich form of periodic, quasi-periodic and chaotic vibrations. However, most of the previous research was focused on numerical investigations and only a few works were on experimental work. This is partially because it is difficult for the rotor-to-stator rub to be well simulated experimentally. Generally, previous work used some kind of soft metal to contact the rotor to simulate the malfunction. This method has two disadvantages. It cannot simulate the condition of the full rub and in most cases it will lead to serious damage to the shaft.

In our research, an experimental setup was installed to simulate the rub-impact of the rotor system. A special structure of stator was designed that could simulate the condition of the full rub. The experiments were performed under different conditions to observe the nonlinear vibrations. It is expected that some valuable vibration features of the rub-impact rotor system can be observed and the research can provide some useful information for the fault diagnostics of rotating machinery.

2. Experimental setup

The experimental setup is shown in Fig. 1. A coupling is connected between the motor and the shaft. The setup has the characteristics of simple structure, wide speed range, being stable and reliable. The rated current of the electric motor is 2.5 A and the output power is 250 W. The rotating speed can be adjusted between 0 and 10000 rev/min and the rate of the speed increase can reach up to 800 rev/min. The rotating shaft has a diameter of 9.5 mm with two types of length 320 and 500 mm. Any positions along the axial direction can be chosen as the supporting points of the shaft during the experiment. The experimental setup can hold three rotors at its maximum. The eddy current transducers are used to measure the vibration displacements of the rotors. For every rotor, at least one position is chosen to place two transducers in vertical and horizontal directions, respectively. There are rigid, semi-flexible and flexible couplings available for the connections between rotors and between the rotor and the electric motor shaft to meet different experimental requirements.

Previous experimental investigations for the rub-impact rotor systems usually use the way of the point contact. In this manner a rub screw holder is fixed at a certain position. Then the electric motor is started to operate at the experimental speed. The distance between the rub screw and the shaft is adjusted to an appropriate value until the rub impact is observed. Finally, the anti-looseness wing nut is tightened. However, this kind of simulation does not agree with most cases of the real rotor-to-stator rub-impact and the experiment cannot simulate the condition of the full rub. Also the damage to the shaft will be caused in this kind of experiment and the experiment can only last for a short period of time. In order to simulate the real process of the rub-impact better, we have designed a special structure of stator that can make it possible to perform a full rub experiment, as shown in Fig. 2. It is easy for the stator to be installed or detached. The clearance between the rotor and stator is adjustable to meet different experimental conditions.

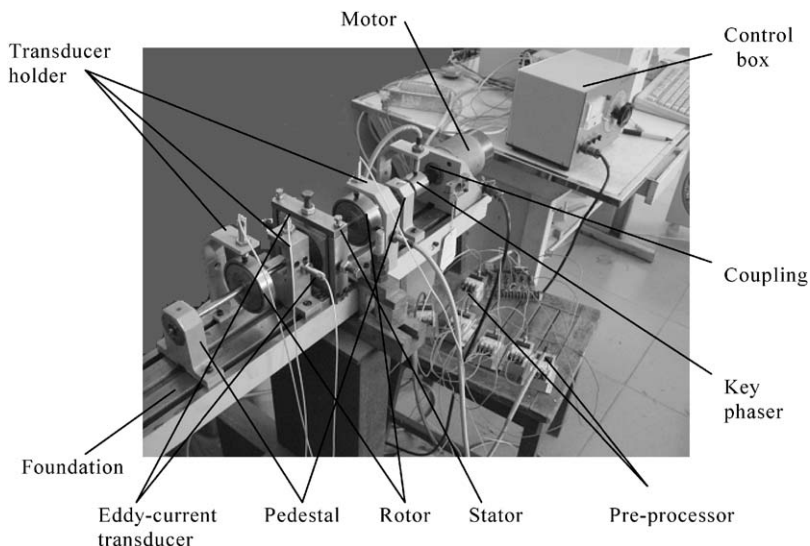


Fig. 1. Experiment arrangement of the rub-impact rotor system.

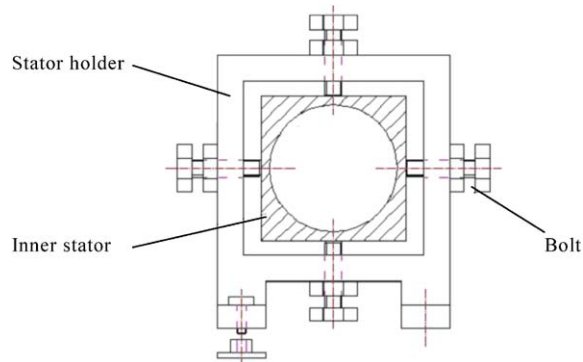


Fig. 2. Diagram of the stator structure.

In order to reduce the wear of the disks, a soft aluminum alloy is used to make the inner part of the stator. Three sizes of the inner stator were designed to simulate different clearances of 0.4, 0.6 and 0.8 mm, respectively. Four bolts were used to fix the inner stator and the stator holder tightly. The holder was a kind of the steel structure to increase the stiffness of the whole stator. Thus not only can the concentricity of the stator and the rotor (uniform clearance along the circumferential direction between the rotor and the stator) be adjusted, but also the size of the clearance can be adjusted by changing the different inner stators to control the time when the rub-impact occurs and the severity of the rubbing.

Experimental vibration data and the key-phasing data can be measured by the eddy current transducers, amplified by the pre-amplifier, received by the data-acquisition card and finally sent to the computer for recording. The data-acquisition card can receive 16 channels of signals simultaneously and its sampling frequency can reach a maximum of 100 kHz. The sampling speed is 1.6 kHz and the rotating speed is controlled to be below 5000 rev/min. When the vibration data needs to be measured at more than three disk positions simultaneously the rotating speed is generally controlled to be below 3000 rev/min.

3. Experiments and result analysis

The influence of the rotor-to-stator rub on the system characteristics is very complicated. The time and position at which it occurs cannot be predicted. During the start and finish periods of the partial rub, sudden appearance and disappearance of the contact will cause a rapid change in the system momentum and therefore leads to an impact on the system. This corresponds to the introduction of a wideband excitation to the system and the complicated transient responses are thus caused in the system. In this case it is very difficult to keep the rub-impact rotor system rotating at a very steady speed. Moreover, besides the large radial interaction, the relative motion caused by the rotation of the rotor can be produced at the contacting point between the rotor and the stator, which will lead to the friction. This will subsequently result in the wear and the thermal effect of the rotor and stator, and causes the thermal deformation to the rotor and the inhomogeneous thermal expansion to the stator. During this process the friction coefficient will be

changed and the unbalance will be increased. This will further make the vibration aggravated and the rub-impact more severe. Therefore long periods of the rubbing will lead to a serious damage of the system.

A large set of parameters could be used to control the motion of the rotor system: the rotating speed, unbalance, the system damping, stiffness, bearing parameter, etc. The commonly used parameter is the rotating speed. The vibration characteristics of the rotor system in the whole starting process can be observed by changing this parameter.

A complete experimental description of all figures is shown in Table 1. Each of the figures contained in Table 1, from the top to the bottom, shows vibration waveforms, spectra, orbits, and Poincaré's maps, respectively; in the vibration forms, abscissa is the period number and the ordinate is the vibration displacement in mm; in the spectra, abscissa is the frequency and ordinate is the spectrum amplitude in mm; in the orbits and Poincaré's maps, abscissa and ordinate are the vibration displacements in mm in the X and Y directions, respectively.

Experiment 1: Single-disk experiment. The experimental rig is with a single disk and with rigid supports. The parameters are: $m=0.6116$ kg, $l=0.380$ m, imbalance $u_x=6.8 \times 10^{-5}$ m, $u_y=7.1 \times 10^{-5}$ m. The inner diameter of the stator is 76.72 mm and the outer diameter of the disk is 76.2 mm. The rub-impact occurs at a rotating speed of 2600 rev/min and the first natural frequency of the system is around 2800 rev/min.

Figs. 3–5 show the vibration waveforms, spectra, orbits and Poincaré's maps of the rotor system as the rotating speed changes. The vibration signals were recorded from $\omega = 1351$ rev/min to 3030 rev/min. A complete process, from no rub-impact to having rub-impact, from slight rub to serious rub, can be observed during this speed range. When $\omega = 1351$ rev/min, vibration amplitude is very small, much smaller than the static clearance between the rotor and the stator. Therefore no rub-impact occurs in this case. However, the vibration waveform is not yet a sine-cosine curve because of the influence of other factors, such as noise and misalignment, as

Table 1
A description of experiment

Experiment	Structure description	Figures concerned	Rotating speeds shown (rev/min)
1	One-rotor, single-disk	Fig. 3 Fig. 4 Fig. 5	$\omega = 1351, \omega = 2500, \omega = 2600$ $\omega = 2631, \omega = 2702, \omega = 2777$ $\omega = 2800, \omega = 2857, \omega = 3030$
2	One-rotor, three-disk	Fig. 6	$\omega = 2857, \omega = 4347, \omega = 4761$
3	Two-rotor, one-disk	Fig. 8 Fig. 9	$\omega = 3448, \omega = 3449, \omega = 3571$ $\omega = 3703, \omega = 4000, \omega = 4167$
4	Two-rotor, multi-disk	Fig. 11 Fig. 12 Fig. 13 Fig. 14 Fig. 15 Fig. 16	$\omega = 1562, \omega = 1694, \omega = 2040$ $\omega = 4761, \omega = 5000, \omega = 5283$ $\omega = 1449, \omega = 1639, \omega = 1923$ $\omega = 4300, \omega = 4540, \omega = 5000$ $\omega = 1282, \omega = 1538, \omega = 1818$ $\omega = 2127, \omega = 2631, \omega = 3500$

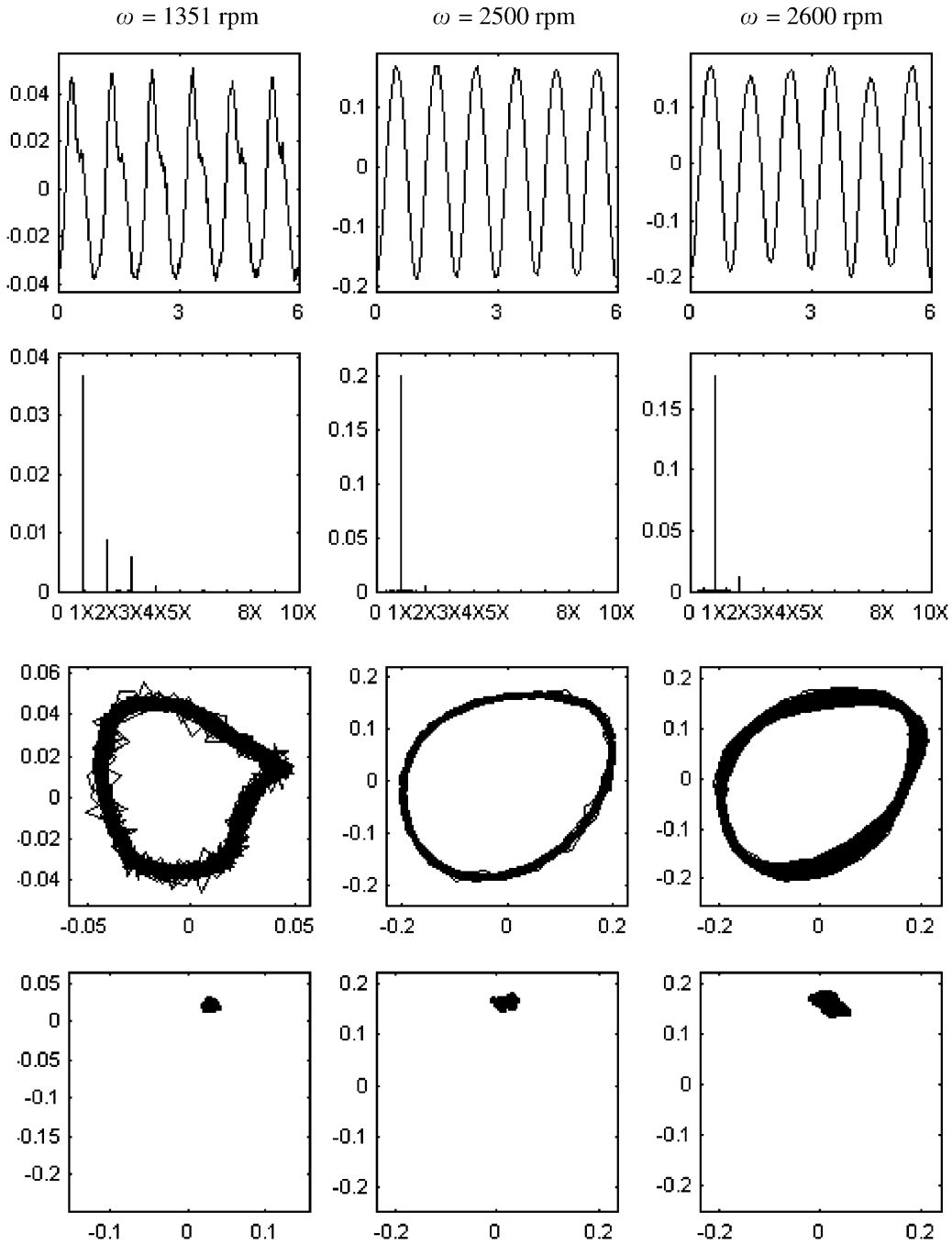


Fig. 3. Experimental results of the rub-impact rotor system for Experiment 1.

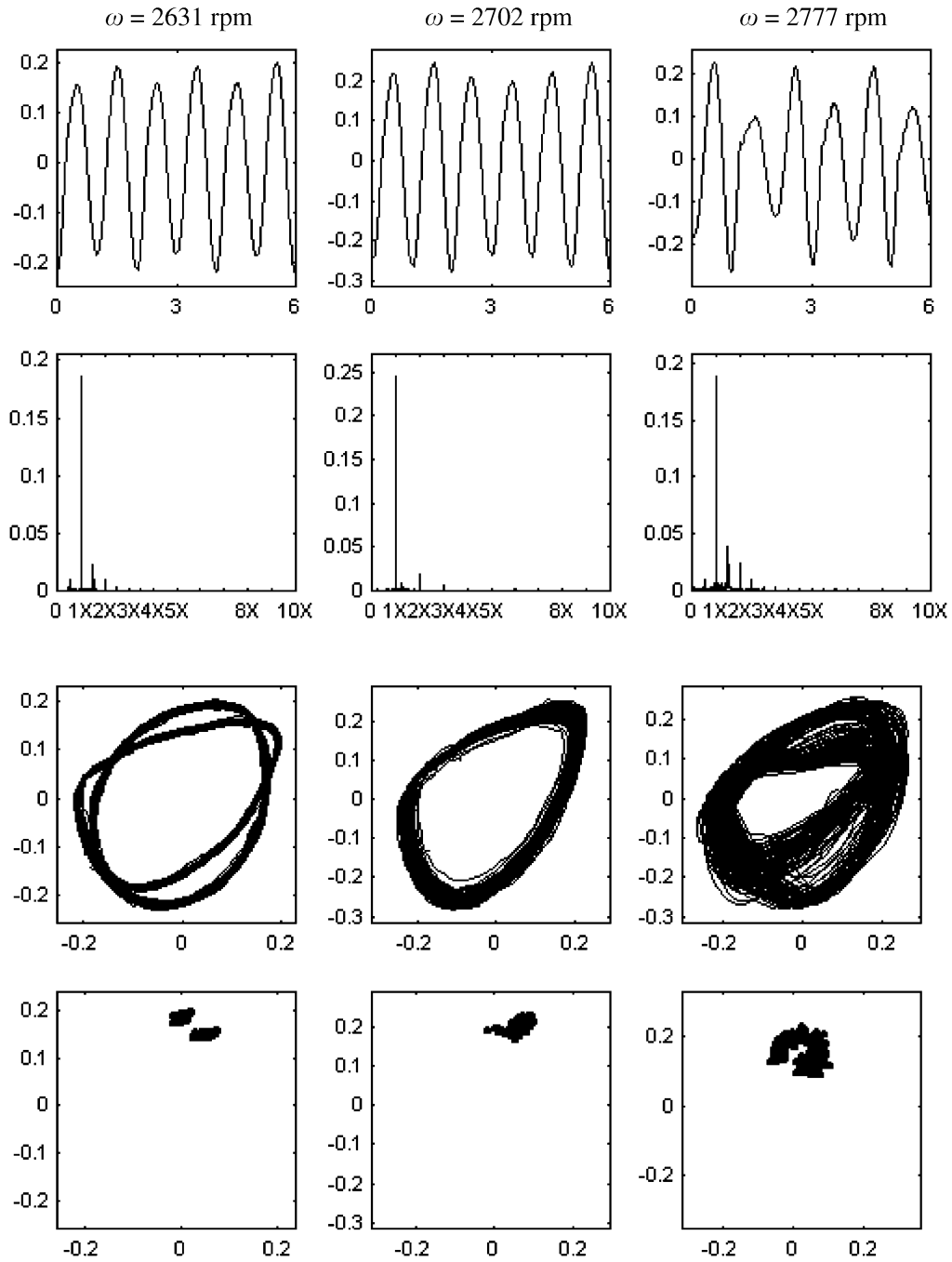


Fig. 4. Experimental results of the rub-impact rotor system for Experiment 1.

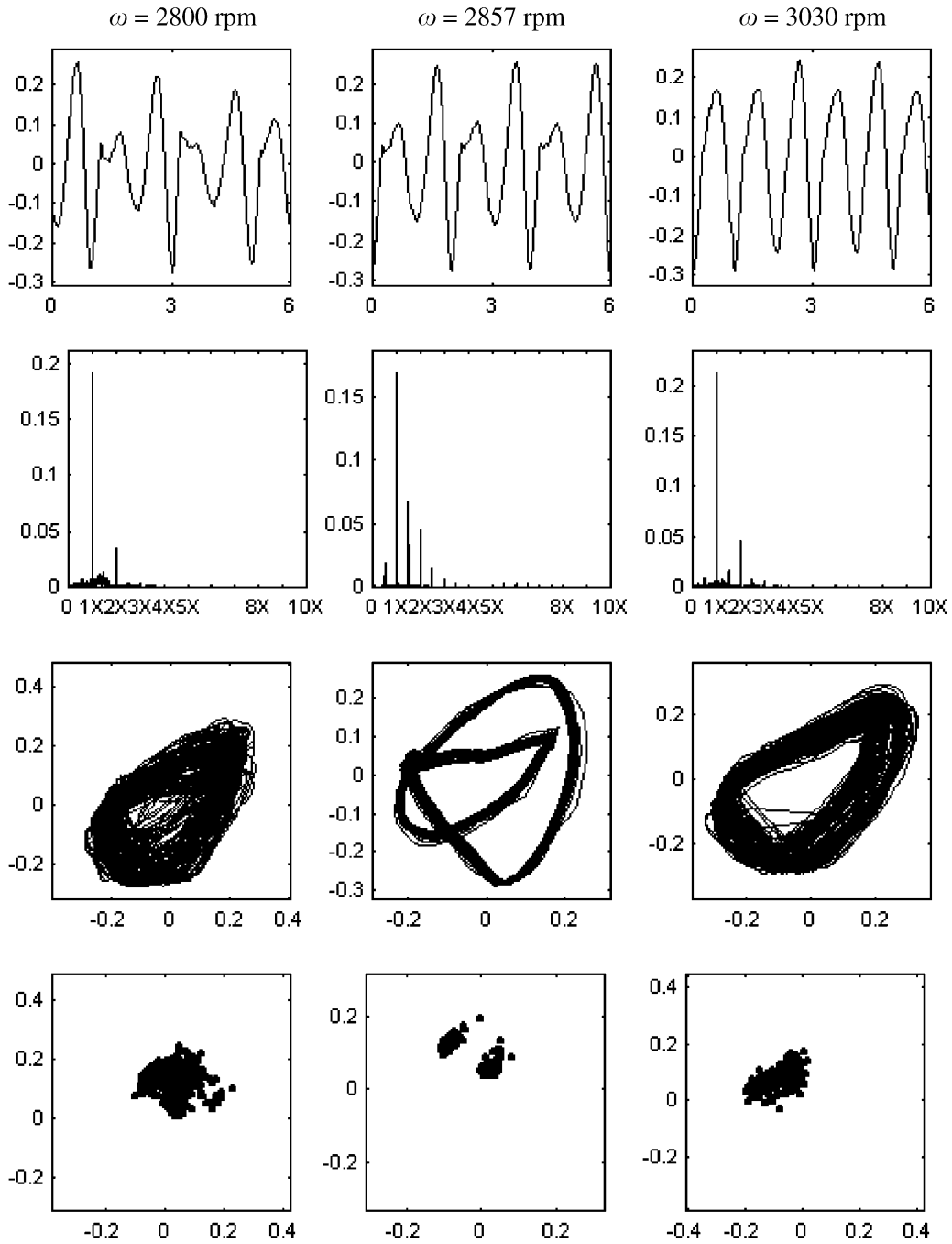


Fig. 5. Experimental results of the rub-impact rotor system for Experiment 1.

shown in the waveforms and orbits. At $\omega = 2500$ rev/min, vibration amplitudes are quite big and reach at a value of 0.2 mm. It can be seen from the waveforms and orbits that there is little influence of noise and misalignment. It can also be clearly seen from the spectrum that a single spectrum line can be observed at the position of the rotating speed and basically zero at other positions. Therefore, this is the typical vibration response for the case of no rub-impact. When the rotating speed is increased to $\omega = 2600$ rev/min, there is some sign of slight rubbing in the orbits. 2X component can be clearly seen from the spectrum except the 1X component. There is only one single point in Poincaré's map which indicates that the system motion is period-one. At $\omega = 2631$ rev/min, not only the rub-impact but also the bifurcation phenomenon can be observed. The spectrum shows the 1/2 fractional harmonic components, such as 1/2X, 3/2X, etc. Certainly the 2X component is still big. The orbits show two circles and Poincaré's map has two points. Therefore the rotor has a period-two motion. When $\omega = 2702$ rev/min, 1/4X, 3/4X and 5/4X components can be observed in the spectrum and the vibration waveforms and orbits are still quite regular. Some changes can be seen when the rotating speed is increased to 2777 rev/min. In this case the vibration waveforms in some periods are not so regular which indicates that the rub-impact has become more serious. The 1/2X, 3/2X, 4/2X and 5/2X components in the spectrum are bigger than those in the previous cases and the amplitude of the 3/2X component in the spectrum is only the second big to that of the 1X component. The continuous spectrum can be found near the 1X component. It can also be seen from the orbits and Poincaré's map that although the orbits have some features of periodic motion but Poincaré's map has shown some form of chaotic state. When the rotating speed has arrived at 2800 rev/min, clearly chaotic features can be observed. Truncation of the vibration waveform has become more obvious. The continuous spectrum can be observed. Poincaré's map indicates that the system is in the state of chaotic motion. At 2857 rev/min, the period-two motion is again resumed. Compared with the previous period-two motion, the rub-impact is more serious in this case and large 1/2X, 3/2X, 4/2X, 5/2X and other components are accompanied. At 3030 rev/min, the system response characteristics are very similar to those in $\omega = 2777$ rev/min. But in the frequency composition, the amplitude of the 2X component is the second next to that of the 1X component and the amplitudes of 1/2X and 3/2X components are also significant. The continuous spectrum can be observed near the 1X component and the motion is clearly chaotic. After this rotating speed, the system is approaching its critical speed. When the motion has passed the critical speed, the amplitude of the vibration has suddenly become small. The rub-impact interaction cannot be observed within the subsequent large speed range. It can be concluded from the whole process that as the rotating speed is increasing, the rub-impact rotor system has experienced from the small vibration amplitudes to large, from no rubbing through slight rub-impact to more serious rub-impact, and from period-one (P1) motion through P2, chaotic, P2, and finally to chaotic. The rub-impact has a stiffening function, thus increasing the critical speeds of the system. The first critical speed has therefore been increased from around 2800 to about 3050 rev/min. The rub-impact process has resulted in the 1/2X, 3/2X, 5/2X and other components mainly, 2X, 3X, and other multiple harmonic components, and 1/4X, 5/4X and other fractional harmonic components as well.

Experiment 2: Three-disk experiment. The experimental rig is with three disks and with rigid supports. The parameters are: $m_1 = 0.817$ kg, $m_2 = 0.6116$ kg, $m_3 = 0.614$ kg, $l = 0.500$ m. The

inner diameter of the stator is 76.72 mm and the outer diameter of the disk is 76.2 mm. The rub-impact occurs at the position of the middle disk. The first natural frequency of the system is around 2000 rev/min.

Fig. 6 is the experimental result of the vibration responses at the position of the middle disk as the rotating speed increases. After passing through the first natural frequency quickly, the sound of the rubbing can be clearly heard during the experiment at $\omega = 2857$ rev/min. However, it can be seen from the vibration waveform and the orbit that the vibration amplitudes are still small and the disk and the stator do not show clear rubbing. But we still can see that the vibration waveform is not a very regular sine curve and the orbit shows some kind of triangle. These are the phenomena occurring often during the rotor-to-stator rub. After checking the real condition it is found that because of the misalignment and insufficient lubrication oil in the bearing, the rubbing has occurred between the shaft and the bearing. The rubbing sound heard during the experiment is actually from the bearing and the shaft. The clear 2X component can also be seen from the spectrum. After the rotation of the rotor has been stopped we have touched the bearing and the adjacent shaft by hand and found that they were very hot. And clearly the heat is from the rubbing. As the rotating speed is increasing the rubbing between the bearing and the shaft is gradually becoming slight. The orbits now show regular circles. At $\omega = 4347$ rev/min, the orbits are three closed curves and Poincaré's map is three isolated points. The system shows a P3 motion. It can clearly be seen from the spectrum that the motion contains 1/3 fractional harmonic components, such as 1/3X, 2/3X, 4/3X, 5/3X, etc. The spectrum amplitude of the 4/3X component is the second largest to that of the 1X component. The 2X and 3X components can be seen as well. At $\omega = 4761$ rev/min, the rub-impact becomes more serious. Although the vibration waveform is nearly the same as that in the case of 4347 rev/min, the orbits show very irregular and Poincaré's map is not several isolated but two dense points. This indicated that the system showed some chaotic behavior. It can be seen from the spectrum that besides the 1/3X fractional harmonic components such as 1/3X, 2/3X, 4/3X, 5/3X, etc. the amplitude of 2X component is also large. But on the whole, except the 1X component, the 1/3X component dominates in the spectrum. It is indicated that as the rub-impact becomes more serious, the frequency composition is more complicated and at the chaotic state the spectrum is continuous. After passing through 4761 rev/min, the system has arrived at its second natural frequency. After that the vibration amplitudes are quickly becoming small.

Experiment 3: Two-rotor one-disk experiment. As shown in Fig. 7, the motor drives the rotor 1 through a semi-flexible coupling and the latter then drives the rotor 2 through a flexible coupling. In the figure $l_1 = 96$ mm, $l_2 = 22$ mm, $l_3 = 44$ mm. The mass of the disk on the rotor 2 is $m = 0.817$ kg. A mass unbalance of 3 g is added at a position of 33 mm to the center of the disk (equivalent unbalance of 1.209×10^{-4} m). The inner diameter of the stator is 76.72 mm and the outer diameter of the disk is 76.2 mm.

The first natural frequency of the system is around 2400 rev/min (40 Hz). Figs. 8 and 9 are the experimental results of the rub-impact rotor system as the rotating speed increases. It can be seen from the vibration waveforms and the orbits that the rub-impact does not occur at 3448 rev/min. From 3449 through 3571, 3703 to 4000 rev/min the rub-impact is gradually becoming serious and at 4167 rev/min it has become very serious. This trend of change can also be seen from the

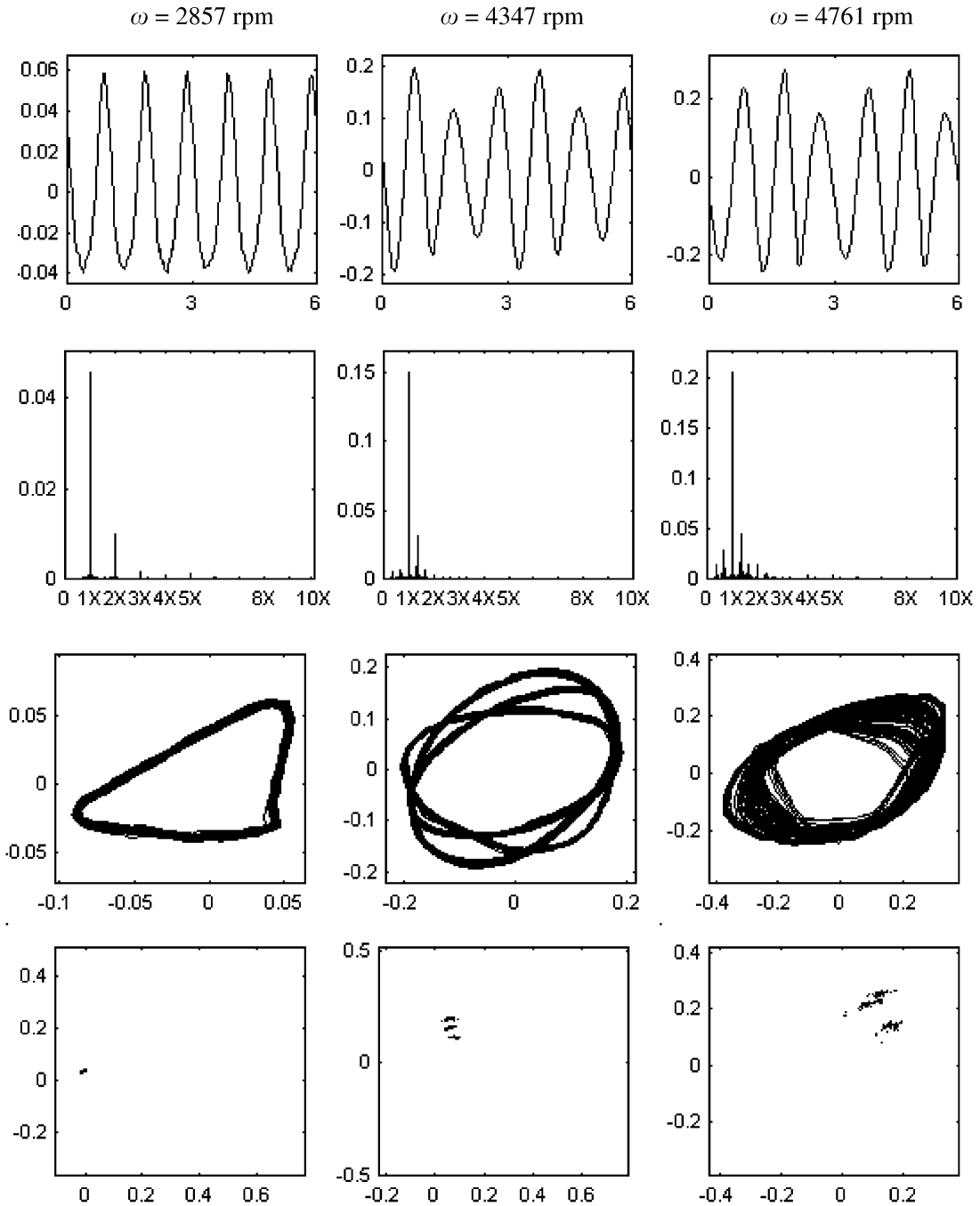


Fig. 6. Experimental results of the rub-impact rotor system for Experiment 2.

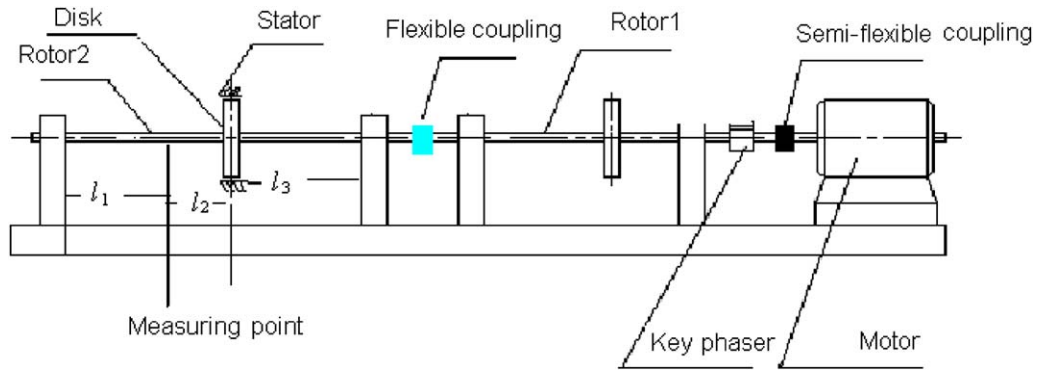


Fig. 7. Diagram of the experimental setup.

spectrum. At the beginning, only the 1X component is evident and the amplitudes of other components are very small. As the rotating speed increases, the frequency components such as $1/2X$, $3/2X$, and $2X$ appear in the spectrum and these components are gradually becoming larger. At 4167 rev/min the spectrum amplitude of the $3/2X$ component is nearly one third of that of the 1X component. Meanwhile Poincaré's map shows one isolated point at 3448 rev/min, two isolated points at 3449 rev/min, then one isolated point again at 3571 rev/min, two isolated points, and finally chaotic status. It can be observed from the spectrum that the main frequency components are $1/2X$, $3/2X$ and $2X$, and the other more complicated components such as $1/3X$, $2/3X$, etc. do not appear.

Experiment 4: Two-rotor multi-disk experiment. As shown in Fig. 10, the motor drives the rotor 1 through a semi-flexible coupling and the latter then drives the rotor 2 through a flexible coupling. In the figure $l_1 = 96$ mm, $l_2 = 98$ mm, $l_3 = 83$ mm, $l_4 = 103$ mm, $l_5 = 55$ mm. The masses of the disks on the rotor 2 is $m_1 = 0.6128$ kg, $m_2 = 0.6143$ kg, $m_3 = 0.817$ kg. The inner diameter of the stator is 76.72 mm and the outer diameter of the disk is 76.2 mm. The first natural frequency of the system is around 1700 rev/min (28 Hz). The rub-impact occurs at the position of m_2 of the rotor 2.

Figs. 11 and 12 are the experimental results of the rub-impact rotor system as the rotating speed increases under the condition that no imbalances are added on three disks. It can be seen that the whole process is from no rub-impact, through slight, then serious rub-impact, and finally to the chaotic state. However, we can also observe some results different from previous experiments. At 1694 rev/min, some fractional harmonic components such as $1/2X$, $3/2X$, etc. can be observed while at 2040 rev/min the $3X$ component with large amplitude can be found. At 5000 rev/min the spectrum amplitude of the $1/2X$ component is larger than that of the 1X component. The chaotic motion can be observed at 5283 rev/min where although the 1X component is still large the whole spectrum has become continuous.

Figs. 13 and 14 are the experimental results of the rub-impact rotor system as the rotating speed increases, in which a mass unbalance of 3 g is added at a position of 33 mm to the center of the

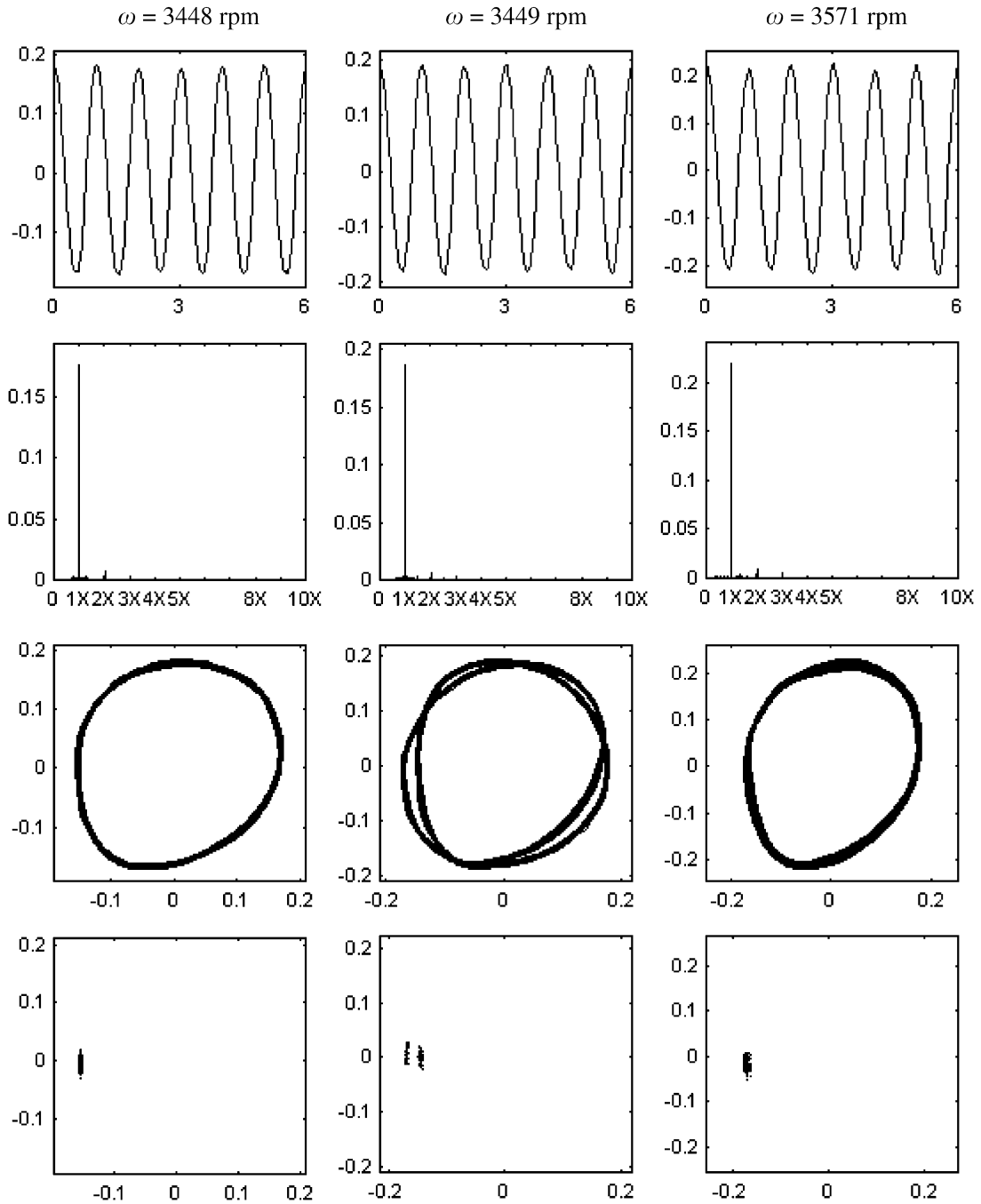


Fig. 8. Experimental results of the rub-impact rotor system for Experiment 3.

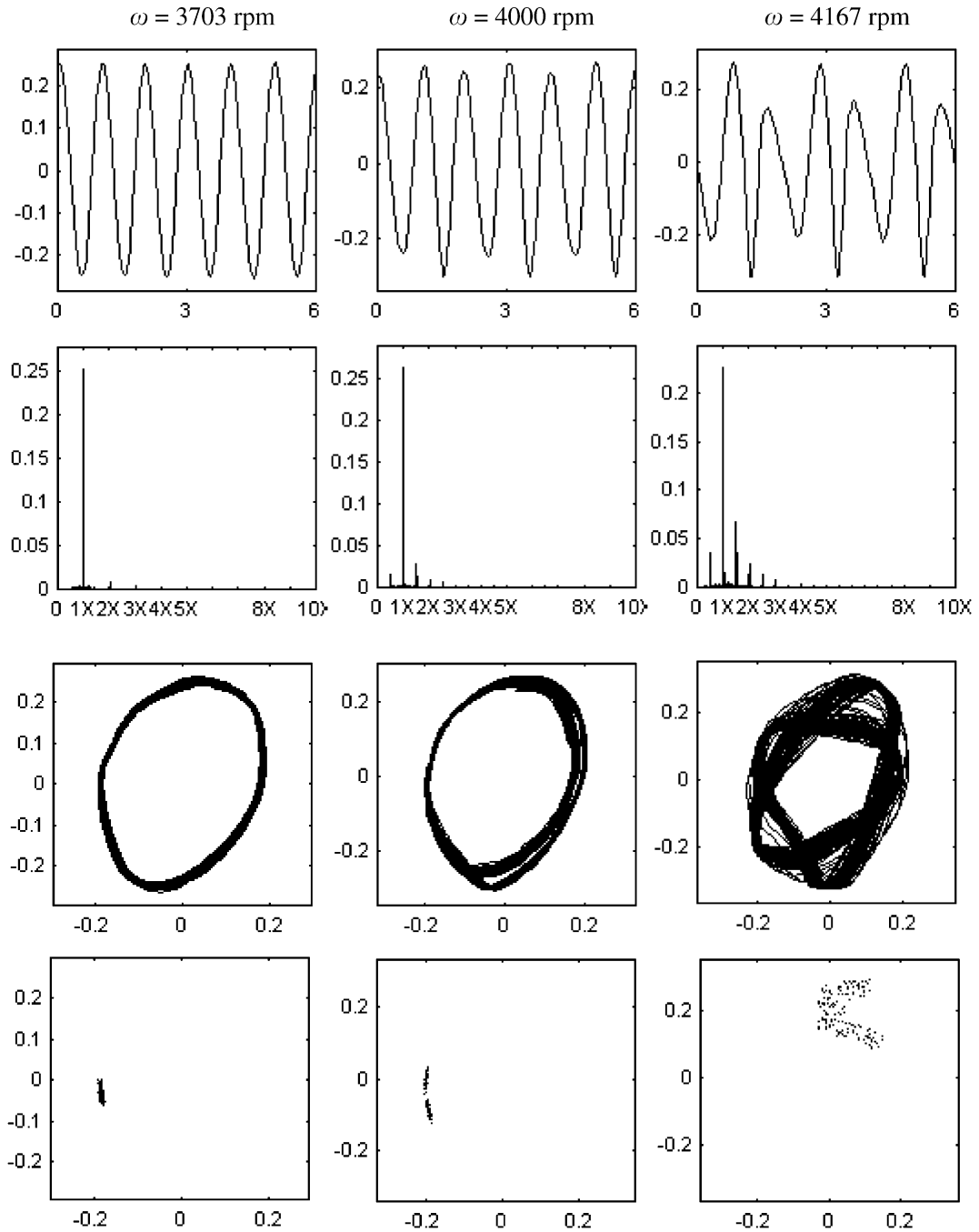


Fig. 9. Experimental results of the rub-impact rotor system for Experiment 3.

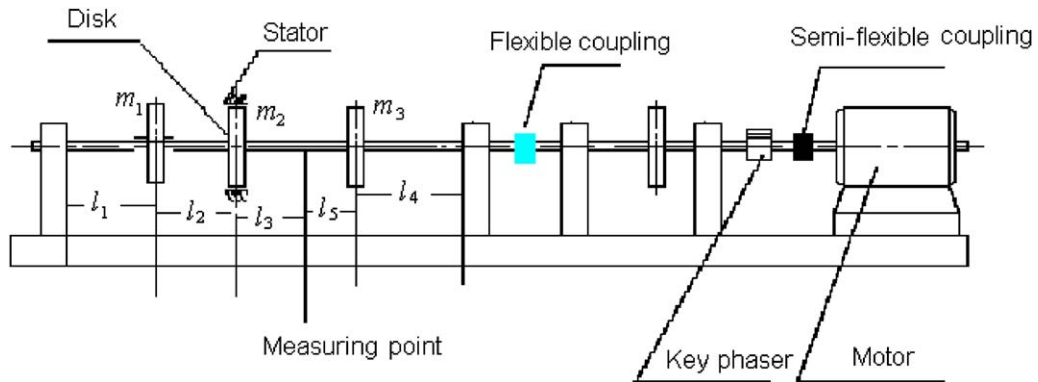


Fig. 10. Diagram of the experimental setup.

disk m_3 . Figs. 15 and 16 are the experimental results where a mass unbalance of 3 g is added at a position of 33 mm to the center of the disk m_2 . The whole rub-impact process is similar to the previous case. When the rub-impact occurs the fractional harmonic components such as $1/2X$, $3/2X$, etc. and the multiple harmonic components such as $2X$, $3X$, etc. can be observed. In the case of disk m_3 with unbalance mass, the system motion becomes chaotic at about 4540 rev/min and enters into quasi-periodic at around 5000 rev/min. And in the case of disk m_2 with unbalance mass, the chaotic motion is at about 2631 rev/min and the quasi-periodic at around 3500 rev/min.

4. Conclusions

In this research an experimental setup of a rub-impact multi-disk rotor system is established. A special structure of stator is designed that can simulate the condition of the full rub. The vibration waveforms, spectra, orbits and Poincaré's maps are used to analyze nonlinear responses and bifurcation characteristics of the system when the rub-impact occurs. The rotating speed is changed as a control parameter to observe the nonlinear vibrations of the system. It is found that in most experiments, when the rub-impact occurs, besides the multiple harmonic components such as $2X$, $3X$, etc. the $1/2$ fractional harmonic components such as $1/2X$, $3/2X$, etc. can be observed. Under some special cases, besides the multiple harmonic components such as $2X$, $3X$, etc. and the $1/2$ fractional harmonic components such as $1/2X$, $3/2X$, etc. the $1/3$ fractional harmonic components such as $1/3X$, $2/3X$, etc. can be observed as well. As the rub-impact is aggravated, the spectrum composition becomes more complicated and when the rub-impact becomes more serious, the chaotic motion can be observed in all the experiments. Under some special conditions the quasi-periodic vibration can be found. For the chaotic motions, the continuous spectrum can be seen. We have tried but could not trace the routes to and out of chaos because of the difficulty in the accurate control of the rotating speed.

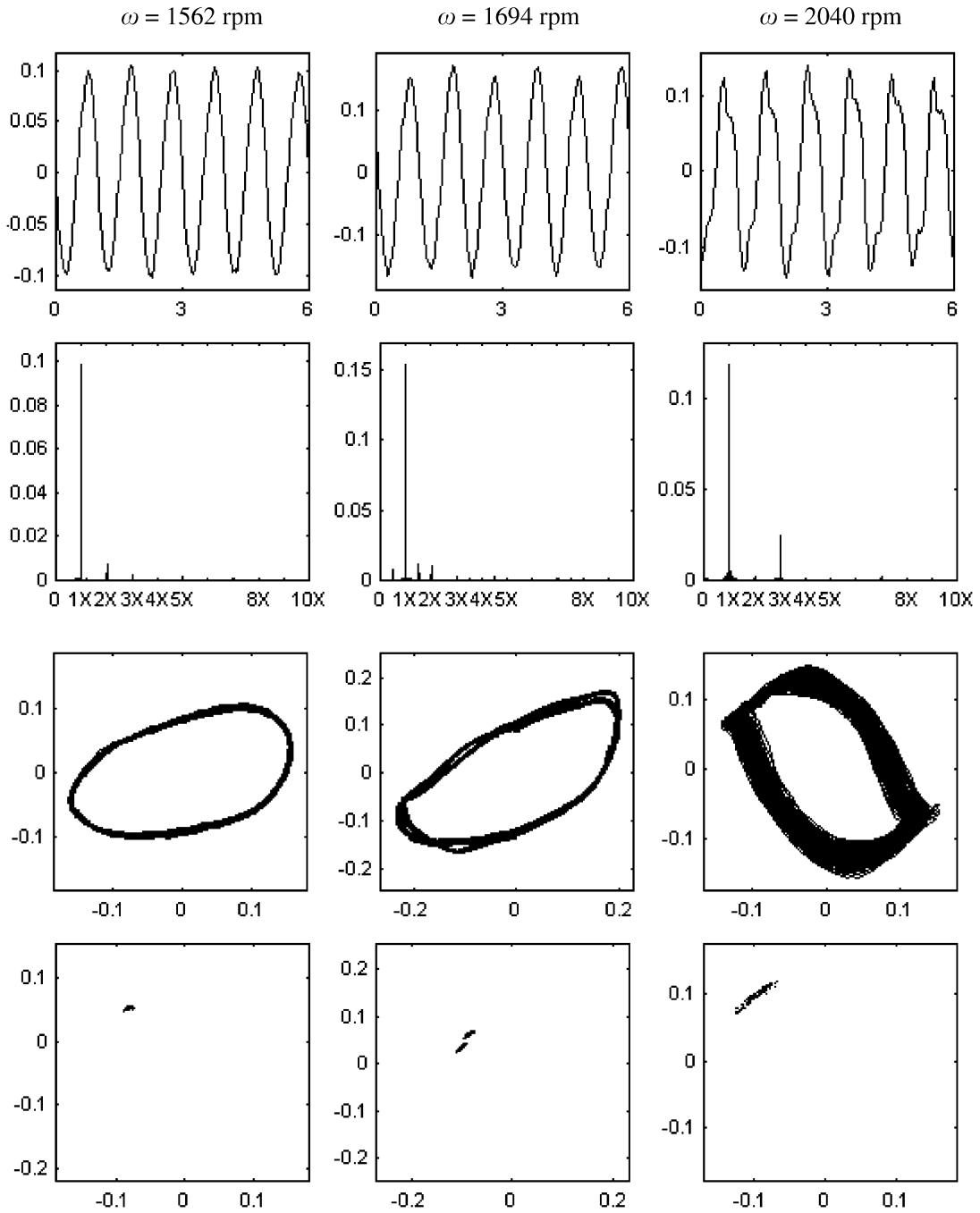


Fig. 11. Experimental results of the rub-impact rotor system for Experiment 4.

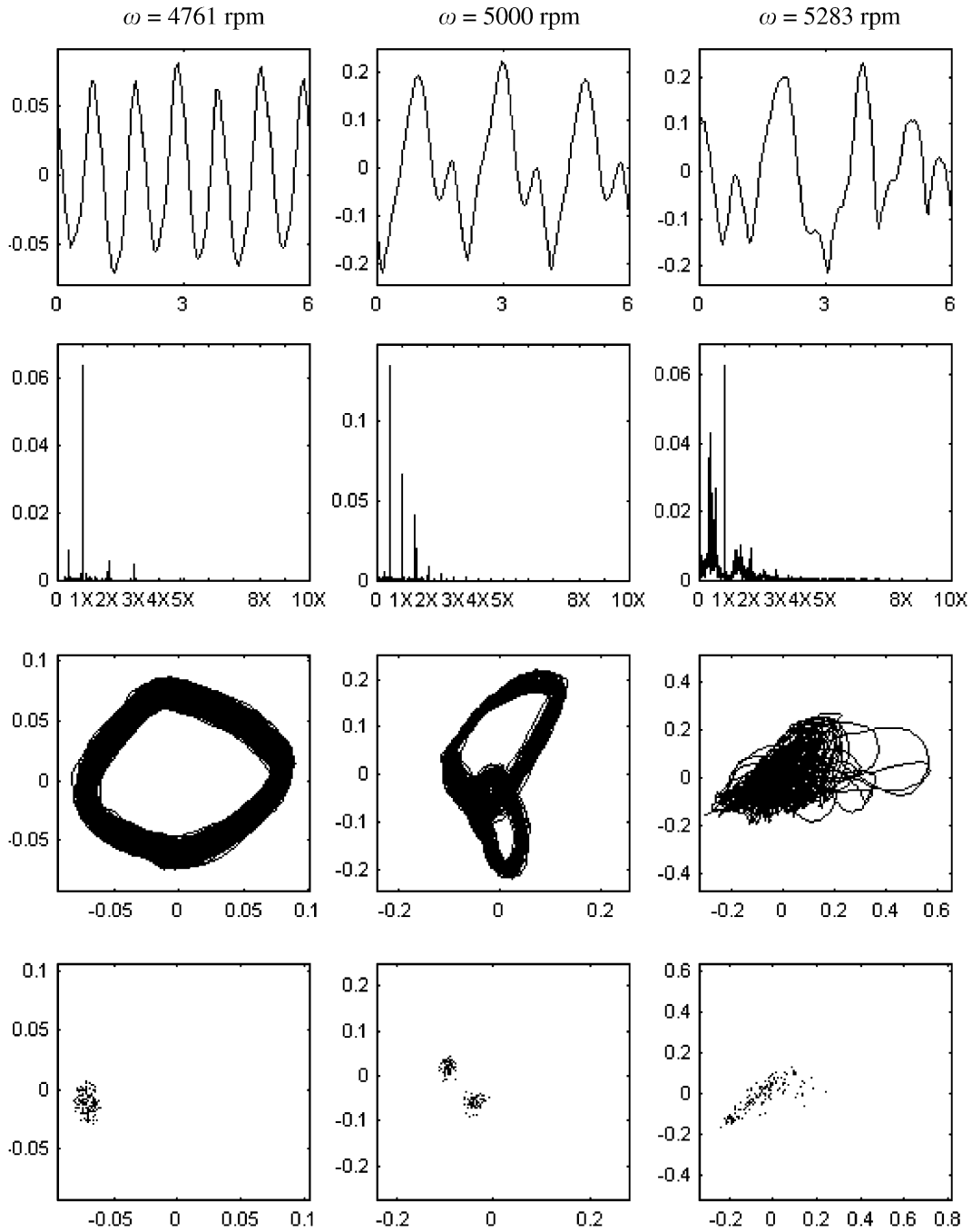


Fig. 12. Experimental results of the rub-impact rotor system for Experiment 4.

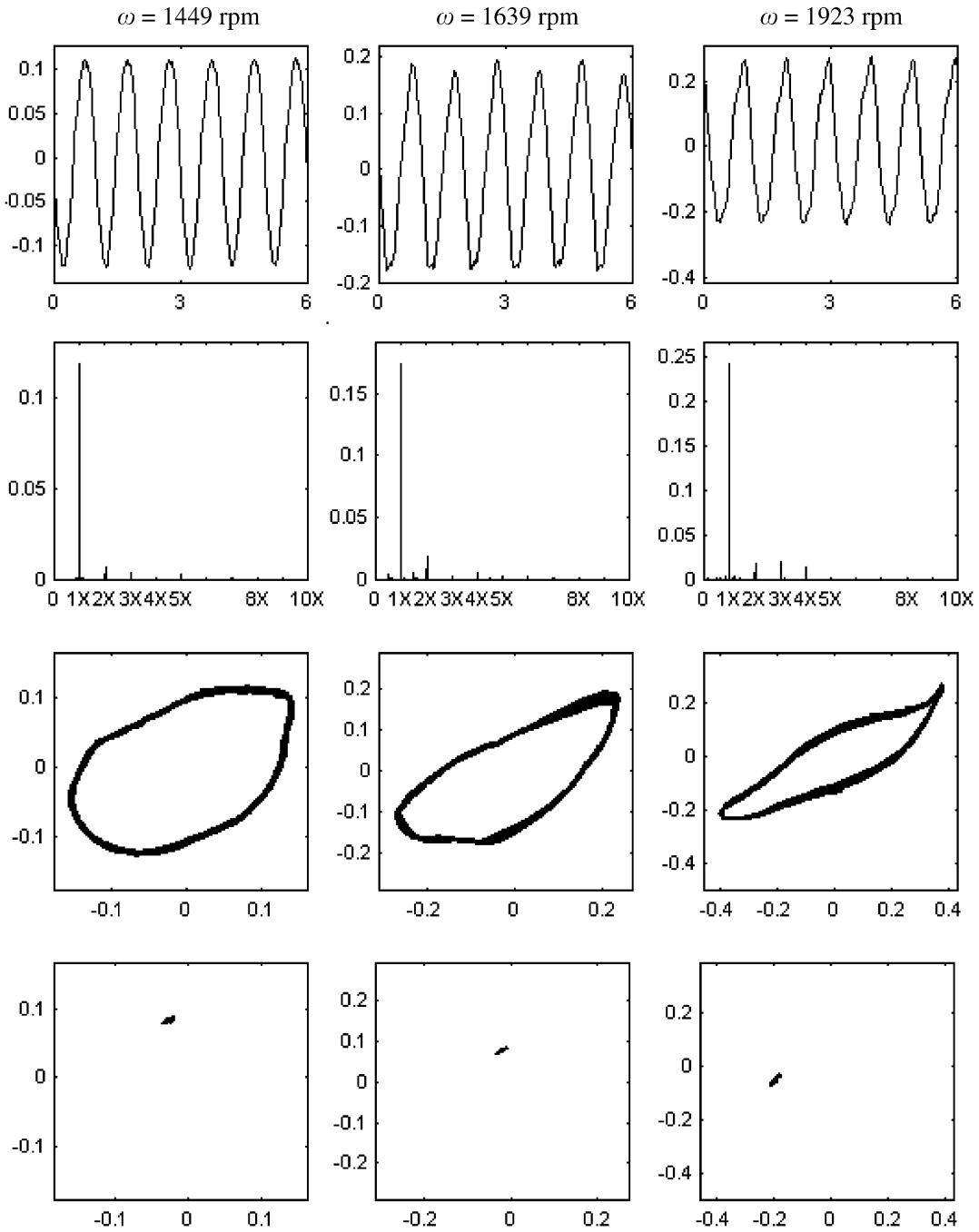


Fig. 13. Experimental results of the rub-impact rotor system for Experiment 4.

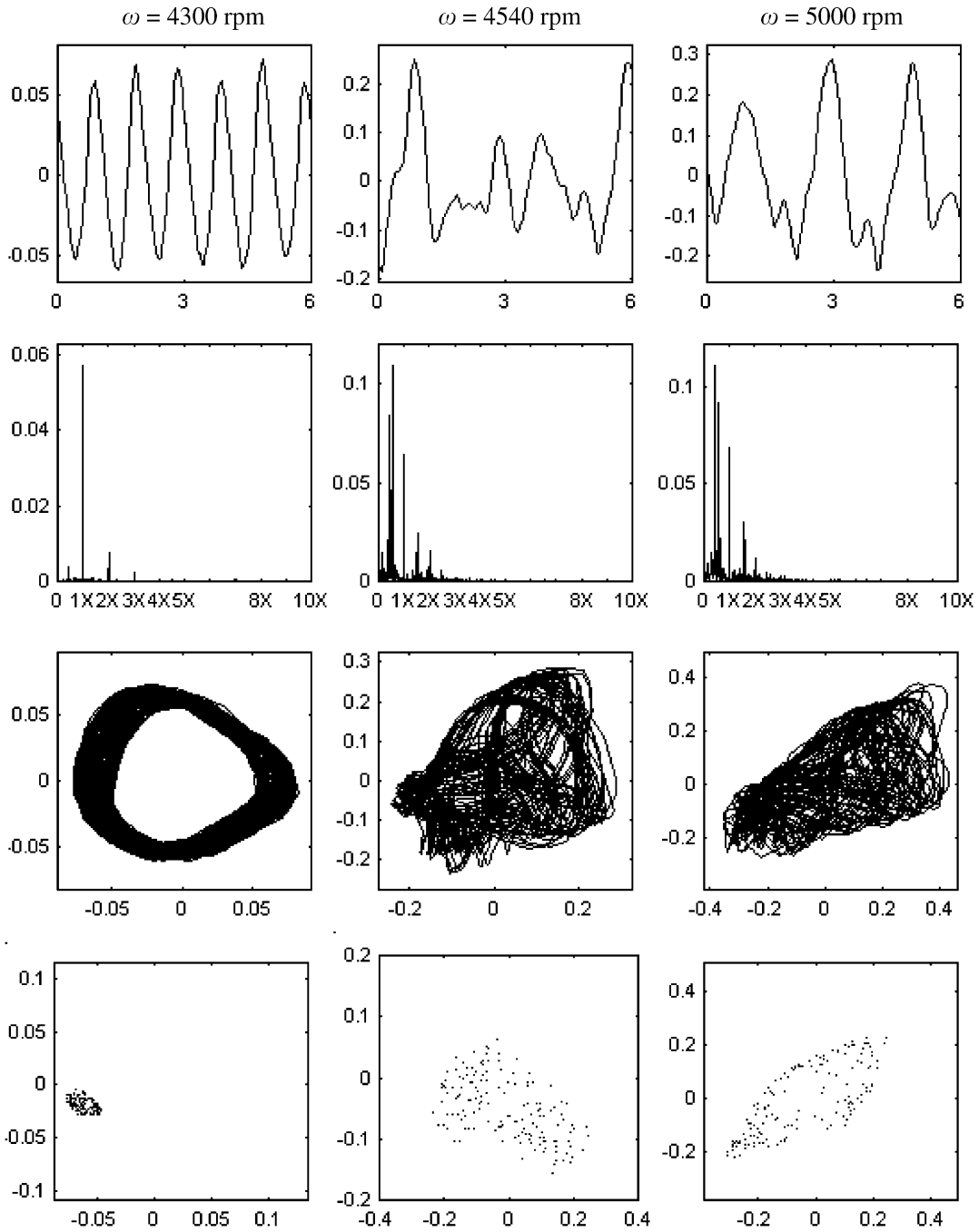


Fig. 14. Experimental results of the rub-impact rotor system for Experiment 4.

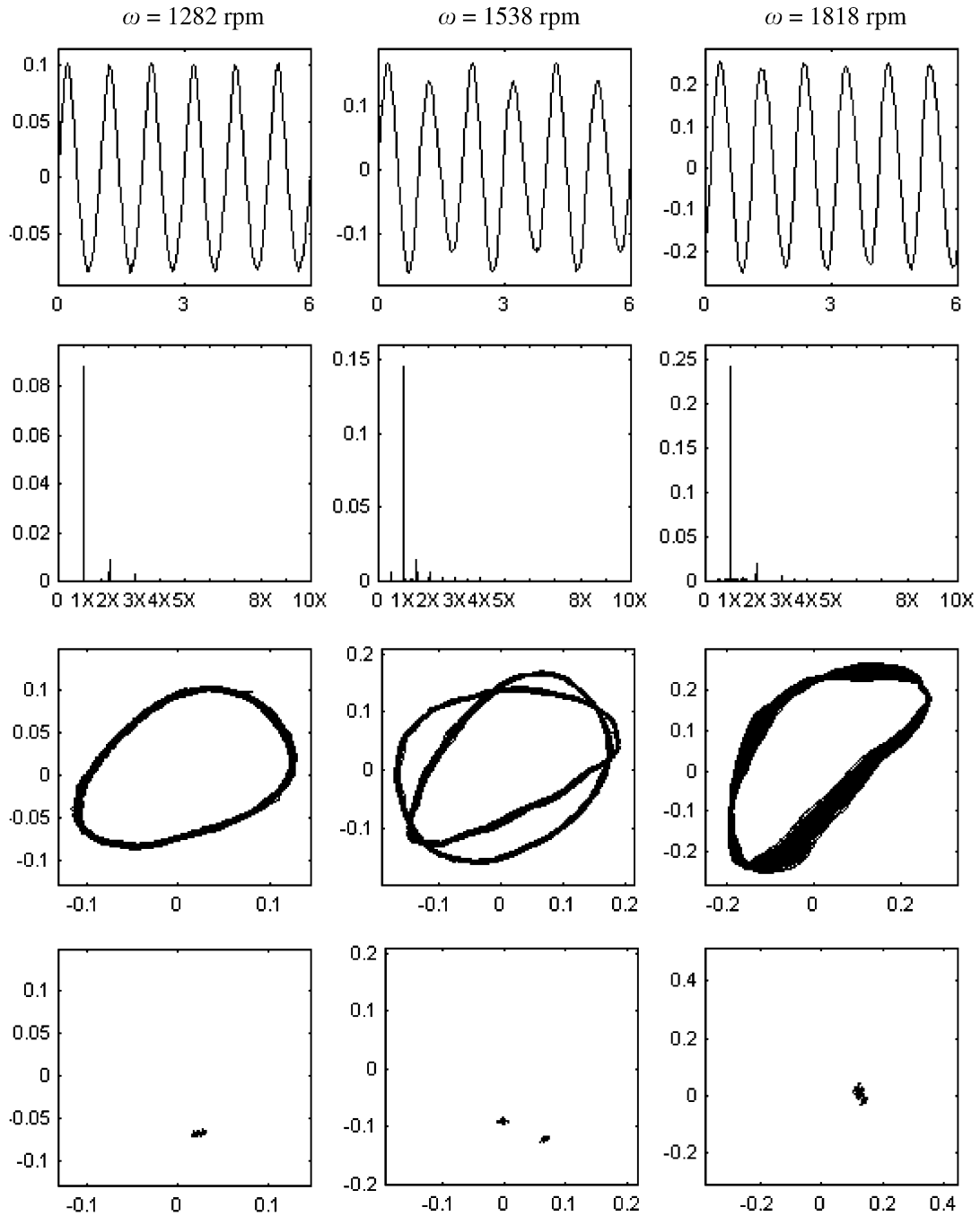


Fig. 15. Experimental results of the rub-impact rotor system for Experiment 4.

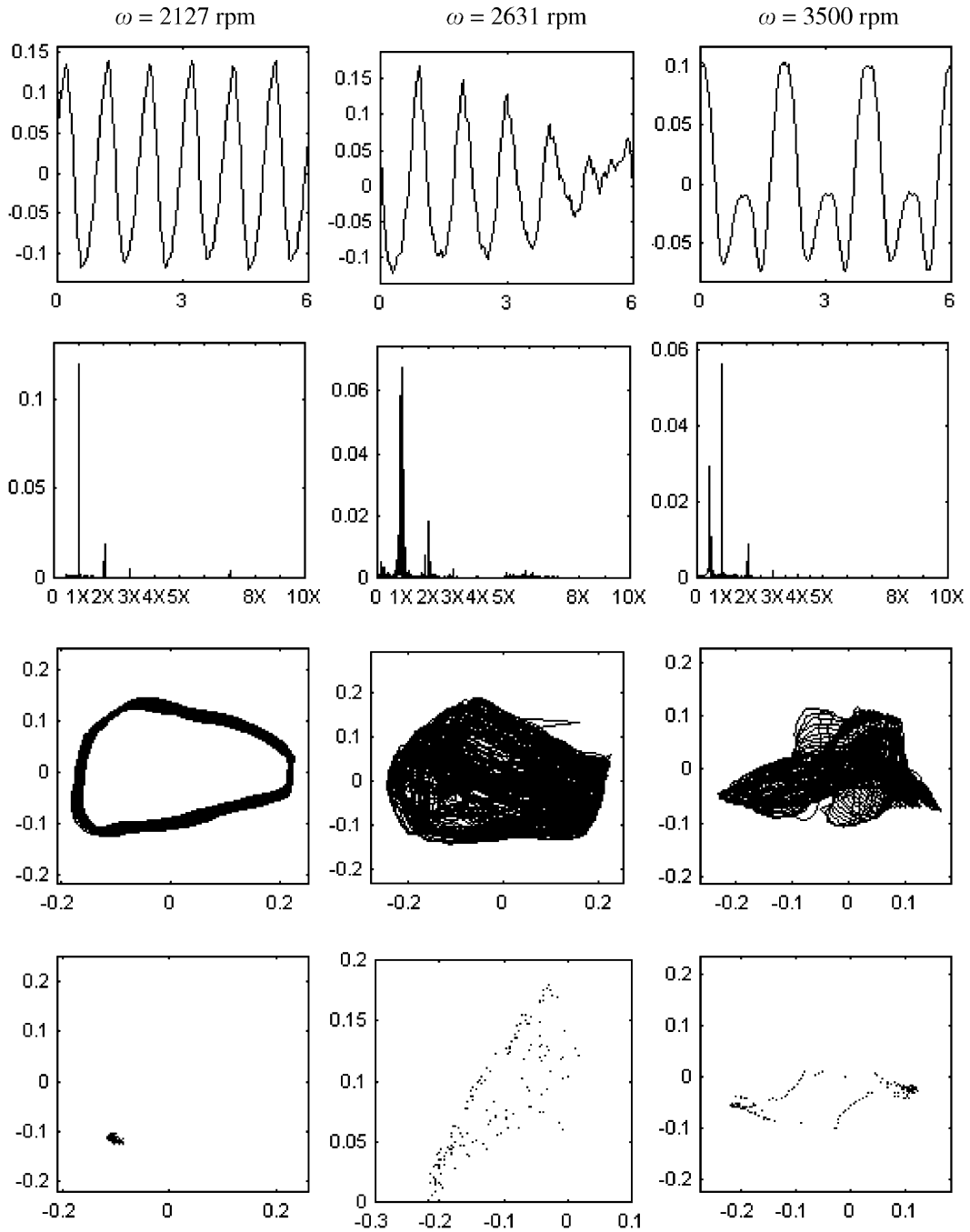


Fig. 16. Experimental results of the rub-impact rotor system for Experiment 4.

Acknowledgements

This research is supported by Natural Science Foundation of China (Grant No. 50375076) and the Trans-Century Training Programme Foundation for the Talents by the Ministry of Education.

References

- [1] A. Muszynska, Rotor-to-stationary element rub-related vibration phenomena in rotating machinery—literature survey, *The Shock and Vibration Digest* 21 (1989) 3–11.
- [2] R.F. Beatty, Differentiating rotor response due to radial rubbing, *Journal of Vibration, Acoustics, Stress, and Reliability in Design* 107 (1985) 151–160.
- [3] F.K. Choy, J. Padovan, Non-linear transient analysis of rotor-casing rub events, *Journal of Sound and Vibration* 113 (1987) 529–545.
- [4] F. Chu, Z. Zhang, Bifurcation and chaos in a rub-impact Jeffcott rotor system, *Journal of Sound and Vibration* 210 (1998) 1–18.
- [5] P. Goldman, A. Muszynska, Rotor-to-stator, rub-related, thermal/mechanical effects in rotating machinery, *Chaos Solitons and Fractals* 5 (1995) 1579–1601.
- [6] H.C. Piccoli, H.I. Weber, Experimental observation of chaotic motion in a rotor with rubbing, *Nonlinear Dynamics* 16 (1998) 55–70.
- [7] S. Edwards, A.W. Lees, M.I. Friswell, The influence of torsion on rotor/stator contact in rotating machinery, *Journal of Sound and Vibration* 225 (1999) 767–778.
- [8] B.O. Al-Bedoor, Transient torsional and lateral vibrations of unbalanced rotors with rotor-to-stator rubbing, *Journal of Sound and Vibration* 229 (2000) 627–645.
- [9] Q. Ding, Y.S. Chen, Nonstationary motion and instability of a shaft/casing system with rubs, *Journal of Vibration and Control* 7 (2001) 327–338.
- [10] F. Lin, M.P. Schoen, U.A. Korde, Numerical investigation with rub-related vibration in rotating machinery, *Journal of Vibration and Control* 7 (2001) 833–848.
- [11] X. Dai, Z. Jin, X. Zhang, Dynamic behavior of the full rotor/stop rubbing: Numerical simulation and experimental verification, *Journal of Sound and Vibration* 251 (2002) 807–822.
- [12] Z. Sun, J. Xu, T. Zhou, Analysis on complicated characteristics of a high-speed rotor system with rub-impact, *Mechanism and Machine Theory* 37 (2002) 659–672.
- [13] Z.C. Feng, X.Z. Zhang, Rubbing phenomena in rotor-stator contact, *Chaos Solitons and Fractals* 14 (2002) 257–267.
- [14] N.Q. Hu, X.S. Wen, Chaotic behaviour identification of a rub-impact rotor using short-term predictability of measured data, *Proceedings of the Institution of Mechanical Engineers Part C—Journal of Mechanical Engineering Science* 216 (2002) 675–681.
- [15] Zhang Yanmei, Lu Qishao, Zhang Sijin, Impact bifurcate analysis on a bearing-rotor system with unsteady oil film forces, *Journal of Vibration Engineering* 15 (2002) 68–73 (in Chinese).
- [16] Q. Wang, F. Chu, Experimental determination of the rubbing location by means of acoustic emission and wavelet transform, *Journal of Sound and Vibration* 248 (2001) 91–103.
- [17] F. Chu, W. Lu, Determination of the rubbing location in a multi-disk rotor system by means of dynamic stiffness identification, *Journal of Sound and Vibration* 248 (2001) 235–246.
- [18] Z. Peng, Y. He, Q. Lu, F. Chu, Feature extraction of the rub-impact rotor system by means of wavelet analysis, *Journal of Sound and Vibration* 259 (2003) 1000–1010.
- [19] N. Hinrichs, M. Oestreich, K. Popp, Dynamics of oscillators with impact and friction, *Chaos, Solitons and Fractals* 8 (1997) 535–558.
- [20] C.N. Bapat, Periodic motions of an impact oscillator, *Journal of Sound and Vibration* 209 (1998) 43–60.
- [21] C.J. Begley, L.N. Virgin, Impact response and the influence of friction, *Journal of Sound and Vibration* 211 (1998) 801–818.